

OPEN

# Expansion of Human Pluripotent Stem Cell-derived Early Cardiovascular Progenitor Cells by a Cocktail of Signaling Factors

Sadaf Vahdat<sup>1,2</sup>, Sara Pahlavan<sup>1</sup>, Elena Mahmoudi<sup>1</sup>, Maryam Barekat<sup>1</sup>, Hassan Ansari<sup>1</sup>, Behnaz Bakhshandeh<sup>2</sup>, Nasser Aghdami<sup>3</sup> & Hossein Baharvand<sup>1,4\*</sup>

Cardiovascular progenitor cells (CPCs) derived from human pluripotent stem cells (hPSCs) are proposed to be invaluable cell sources for experimental and clinical studies. This wide range of applications necessitates large-scale production of CPCs in an *in vitro* culture system, which enables both expansion and maintenance of these cells. In this study, we aimed to develop a defined and efficient culture medium that uses signaling factors for large-scale expansion of early CPCs, called cardiogenic mesodermal cells (CMCs), which were derived from hPSCs. Chemical screening resulted in a medium that contained a reproducible combination of three factors (A83-01, bFGF, and CHIR99021) that generated 10<sup>14</sup> CMCs after 10 passages without the propensity for tumorigenicity. Expanded CMCs retained their gene expression pattern, chromosomal stability, and differentiation tendency through several passages and showed both the safety and possible cardio-protective potentials when transplanted into the infarcted rat myocardium. These CMCs were efficiently cryopreserved for an extended period of time. This culture medium could be used for both adherent and suspension culture conditions, for which the latter is required for large-scale CMC production. Taken together, hPSC-derived CMCs exhibited self-renewal capacity in our simple, reproducible, and defined medium. These cells might ultimately be potential, promising cell sources for cardiovascular studies.

Cardiovascular diseases, especially ischemic heart conditions, are considered one of the leading causes of death worldwide. Numerous studies have been conducted to develop novel strategies to increase both patients' quality of life and longevity<sup>1</sup>. Despite these efforts, no effective treatment exists for these patients<sup>2</sup>. Recently, cardiac cell therapy has become a promising approach and may replace commonly used treatments. In this regard, researchers propose the use of different cell sources, including those which have been isolated from both non-cardiac and cardiac origins<sup>3</sup>. Among these various cell sources, adult stem cells isolated from non-cardiac origins such as bone marrow-derived stem cells, could not efficiently differentiate into three major cardiac lineages and their regenerative benefits for cardiovascular diseases remain controversial<sup>4</sup>. However, the majority of these cells appear to be clinically safe and their positive impacts on heart performance are mostly attributed to paracrine effects.

Over the last decade, global attention has turned to cardiac lineage cells such as cardiomyocytes and cardiovascular progenitor cells (CPCs) as promising cell sources for cardiac cell therapy. However, the challenges of *in vitro* culture and the electrical coupling to the host myocardium restrict the application of cardiomyocytes in clinical studies<sup>3</sup>. Therefore, this new area may benefit from a cardiac-committed, preferably autologous cell type that has the capability for *in vitro* expansion, engraftment after transplantation, and differentiation into cardiovascular lineages *in vivo*<sup>5,6</sup>. Development of an *in vitro* culture system for large-scale production and long-term maintenance of cardiac cell types, especially progenitor cells, is in tremendous demand<sup>5</sup>.

CPCs can be generated by *in vitro* differentiation of human pluripotent stem cells (hPSCs) into cardiovascular lineages. CPCs are clonogenic and have self-renewal capacity as well as the ability to differentiate into cardiac

<sup>1</sup>Department of Stem Cells and Developmental Biology, Cell Science Research Center, Royan Institute for Stem Cell Biology and Technology, ACECR, Tehran, Iran. <sup>2</sup>Department of Biotechnology, College of Science, University of Tehran, Tehran, Iran. <sup>3</sup>Department of Regenerative Medicine, Cell Science Research Center, Royan Institute for Stem Cell Biology and Technology, ACECR, Tehran, Iran. <sup>4</sup>Department of Developmental Biology, University of Science and Culture, Tehran, Iran. \*email: [Baharvand@Royaninstitute.org](mailto:Baharvand@Royaninstitute.org)

lineages<sup>5,7</sup>. Until now, hPSC-derived CPCs (SSEA1<sup>+</sup> cells) were used in rodents after myocardial infarction (MI)<sup>8</sup>, non-human primates models<sup>9,10</sup> and human clinical trials<sup>11</sup>, which suggests that they may be promising sources for cardiac regenerative medicine. Moreover, cardiogenic mesodermal cells (CMCs), which are early CPCs, may hold great promise for cardiac regenerative medicine<sup>12,13</sup>. CMCs are characterized by the expression of mesoderm posterior 1 (MESP1) transcription factor and can differentiate into almost all cardiac cell types both *in vitro* and *in vivo*<sup>13–17</sup>. Therefore, the field of cardiac cell therapy can benefit from the establishment of a culture system for maintenance and long-term/large-scale expansion of CMCs<sup>5</sup>.

In the current study, we aimed to introduce a defined, simple, and reproducible protocol for long-term expansion, maintenance, and storage of hPSC-derived CMCs. We screened some cell signaling factors to develop a chemically defined culture medium. Cultured CMCs expanded for more than 10 passages resulting in  $>10^{14}$  cells, and retained their morphology, molecular pattern, and *in vitro* differentiation propensity into cardiac lineages over passages. We observed no tumorigenicity, engraftment of the self-renewed cells, and improved cardiac performance after transplantation into rat ischemic hearts. This culture condition is reproducible and capable of transformation to a carrier-free suspension culture, which is required for large-scale production of CMCs. Our results provide a novel approach for long-term self-renewal and maintenance of early CPCs, which is a fundamental step for commercialization, developmental, tissue engineering, and cell-based clinical studies.

## Results

***In vitro* generation of CMCs.** A suspension culture system was used to expand and differentiate two human embryonic stem cell (hESC) lines (RH5, RH6) and one hiPSC line (iPS) into CMCs as previously described (Fig. 1a,b)<sup>12,18</sup>. Flow cytometry analysis showed that  $83.3 \pm 5.8\%$  of the RH5-CMCs were MESP1<sup>+</sup>. Furthermore,  $87.4 \pm 5.0\%$  MESP1<sup>+</sup> cells were identified in RH6-CMCs and  $83.1 \pm 9.5\%$  in the iPS-CMCs (Fig. 1c). CMC spheroids, generated from all three pluripotent cell lines, expressed cardiac mesoderm markers and cardiac-specific transcription factors *MESP1*, *SSEA1*, *ISL1*, *PDGFRA*, *NKX2.5*, and *MEF2c* (Fig. 1d).

**Screening of signaling pathway factors for long-term expansion of CMCs.** In order to find an efficient defined medium for prolonged culture and self-renewal of CMCs, based on the literature, we selected eight factors that had putative proliferation potential (Table 1). A top-down approach was designed to find the most effective cocktail of factors. RH5-CMC spheroids were dissociated into single cells and cultured adherently in the presence of selected chemicals. The percentage of MESP1<sup>+</sup> cells and the expansion fold were assessed as the two criteria for the cocktail selection (Fig. 2a–d). Initially, different combinations of 8-1 factors (all factors minus one), were used which resulted in the CMCs expansion in 8-D (all factors minus dorsomorphin, named as 7) (Supplementary Fig. S1). Therefore, the 8-D medium was chosen for the next top-down step. Further removal of one chemical from 8-D resulted in a substantial decrease in cell proliferation. The top-down approach was followed by investigating the impact of removing two factors from 7 factor mixture (Fig. 2a). While there were no significant differences between the 7-2 media groups at the first passage, the CMCs showed the highest expansion fold in the absence of IGF1 and ascorbic acid (7-IV, named as 5 in the following steps) at the second passage (Fig. 2a and Supplementary Fig. S1). Serial removal of signaling factors resulted in the selection of the 5-N (4), 4-P (3), and 3-A (2) combinations based on proliferation rate and preservation of the MESP1<sup>+</sup> cell population in the subsequent steps (Fig. 2b–d). To achieve the most efficient cocktail with the least combination of chemicals, 7, 5, 4, 3, and 2 media were compared for population doubling time (PDT) and cumulative total cell count (Fig. 2e,f). The cocktail of 4 and 3 factors had the least PDT (Fig. 2e). Accordingly, 4 and 3 media had the highest cell count after three passages (Fig. 2f). Furthermore, when CMCs were cultured in medium that contained only one chemical, the medium that contained either A83-01, bFGF or CHIR99021 (CHIR) showed larger fold changes of expansion compared to the other five factors (Supplementary Fig. S2). Therefore, three factors cocktail that contained A83-01, bFGF, and CHIR was selected as the most efficient expansion medium, which was denoted as ABC medium.

Then, different concentrations of A83-01 (0.5, 1, and 2  $\mu$ M), bFGF (10, 25, 50, and 100 ng/ml), and CHIR (3, 6, and 12  $\mu$ M) were tested to obtain the optimal concentrations based on the CMC proliferation rate (Supplementary Fig. S3). The increasing A83-01 concentration led to a substantial reduction in cell count. In contrast, higher concentrations of bFGF (100 ng/ml) resulted in increased cell numbers. Similar to A83-01, increasing the CHIR concentration resulted in a significant reduction in cell expansion. These results suggested that 0.5  $\mu$ M A83-01, 100 ng/ml bFGF, and 3  $\mu$ M CHIR (ABC medium) could be the optimal concentrations for expansion of CMCs.

**Preservation of CMC characteristics after passages.** Cultured CMCs in ABC medium showed epithelial-like morphology with co-expressions of MESP1 and Ki67, and generated colonies that had a dome-like appearance (Fig. 3a,b). In order to determine whether cultivation in ABC medium could preserve CMC characteristics over passages, the percentages of MESP1<sup>+</sup> and Ki67<sup>+</sup> cells were assessed at the early (P1–2) and late (P9–10) passages. Flow cytometry results showed that RH5-CMCs were  $80.8 \pm 3.6\%$  positive for MESP1 during the early passages and  $77.7 \pm 5.5\%$  positive at the late passages. RH5-CMCs also had  $72.7 \pm 1.5\%$  Ki67<sup>+</sup> cells during the early passages and  $59.7 \pm 12.4\%$  during the late passages (Fig. 3c). The same expressions of MESP1 and Ki67 were observed in CMCs derived from the RH6 and iPS lines at the early and late passages (Fig. 3c). The cultured cells expressed CD56 (a surface marker for mesodermal progenitors) and PDGFR $\alpha$  (a well-known CMC surface marker) (Fig. 3d). Moreover, the effect of extended proliferation was assessed on chromosome stability by performing cytogenetic analysis on P10 CMCs. The results showed that these CMCs had a normal karyotype (Fig. 3e). CMCs derived from the RH5, RH6, and iPS lines retained their proliferation rate for more than 9 passages, resulting in  $>10^{14}$  cells (Fig. 3f). Although the PDT and expansion fold showed slight differences over the passages, these findings did not statistically differ (Fig. 3g,h). Quantitative RT-PCR showed a similar expression pattern for CMC markers *MESP1*, *SSEA1*, and *PDGFRA*, as well as early CPC transcription factors *ISL1*, *NKX2.5*,

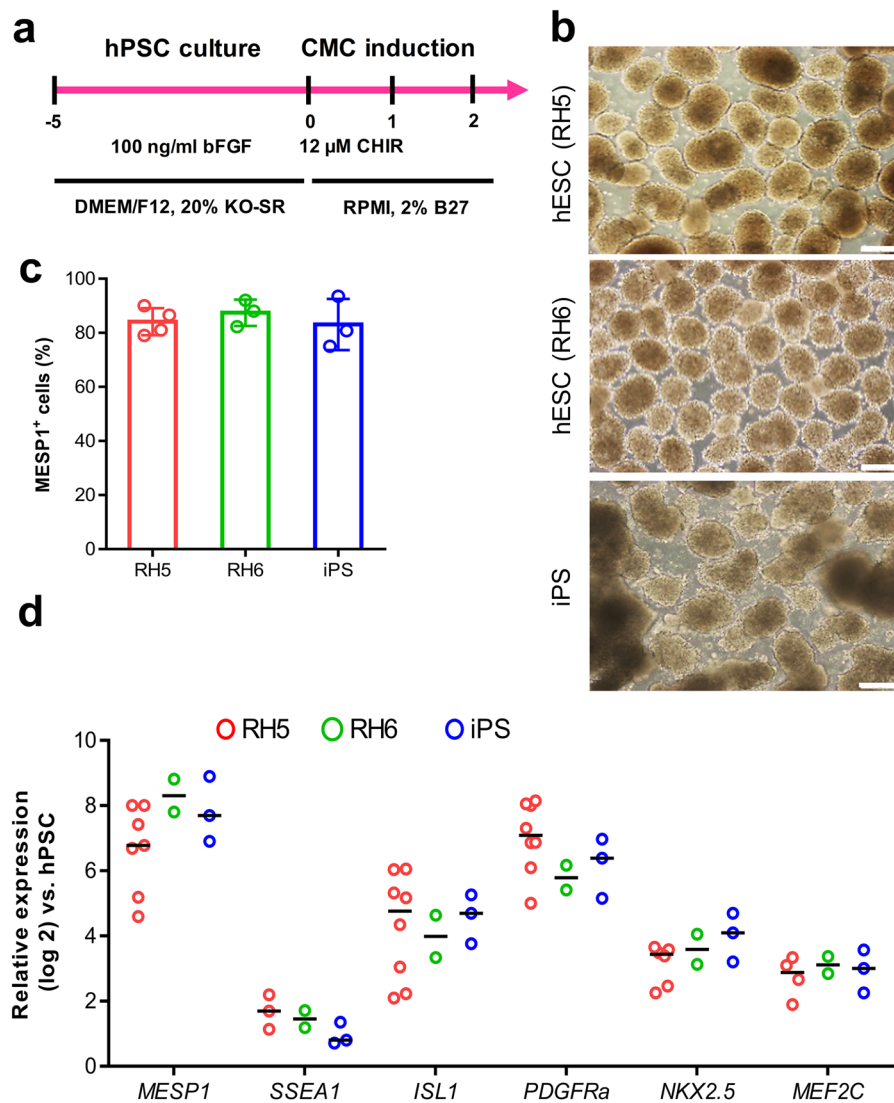


**Figure 1.** Characterization of CMCs generated from three hPSC lines. **(a)** Schematic diagram showing differentiation protocol used for CMC induction from hPSCs. hPSC lines were cultured in suspension as spheroids and differentiated into mesendoderm, followed by cardiac mesoderm lineages by one-day treatment with 12  $\mu$ M CHIR99021 (CHIR) and a one-day rest period. **(b)** Morphology of the CMC spheroids derived from two hESC lines (RH5 and RH6) and an iPS line. Scale bars: 200  $\mu$ m. **(c)** Percentages of MESP1<sup>+</sup> cells in CMC spheroids derived from RH5, RH6, and iPS cells. Data: mean  $\pm$  standard deviation (SD). **(d)** Expression analysis of cardiac mesodermal and cardiac-specific genes in CMC spheroids. Data presented as median.

Candidate factor (abbreviation)	Activity	Reference
A83-01 (A)	Activin/nodal inhibitor	19,26
bFGF (B)	FGF signaling activator	27
CHIR99021 (C)	Wnt signaling activator	19
Dorsomorphin (D)	BMP signaling inhibitor	19
IGF1 (I)	Activation and phosphorylation of Akt and mTOR	28
NRG1 agonist (N)	Potentiating the NRG1/ERBB4 signaling pathway	29
Pioglitazone (P)	PPAR $\gamma$ receptor activator	30
Vitamin C (V)	Chromatin modulator, MEK-ERK1/2 signaling modulator	31

**Table 1.** Candidate signaling factors examined for maintenance and expansion of CMCs.

and *MEF2c* among the passaged and P0 CMCs (Fig. 4a and Supplementary Fig. S4). However, the specific markers of definitive endoderm (*SOX17* and *AFP*) and neural ectoderm (*PAX6*, *TUBB3*, *OLIG2*, and *GFAP*) lineages were downregulated in the early and late passage CMCs (Fig. 4a and Supplementary Fig. S4). Similarly, cultivated

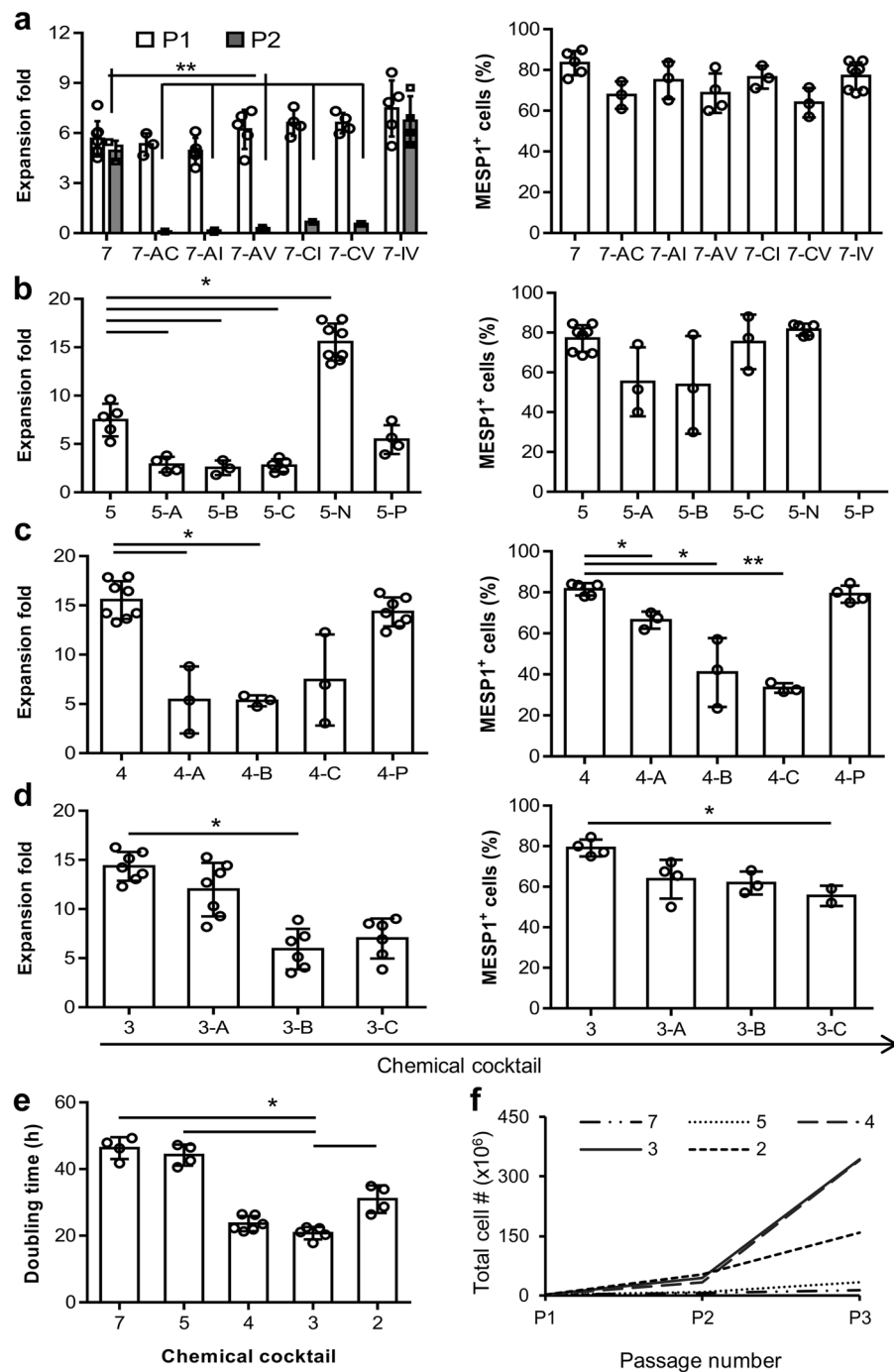


**Figure 2.** A top-down chemical screening to find the most efficient combination of signaling factors for self-renewal of CMCs under adherent culture conditions. (a–d) The expansion fold and percentage of MESP1<sup>+</sup> cells were evaluated as two preliminary criteria to find the minimal essential pool of signaling molecules. In each run, the effect of different combinations of n-1 signaling factors in culture media was assessed according to these criteria. Serial removal of factors resulted in the selection of 7-IV (5), 5-N (4), 4-P (3) and 3-A (2). “-”: Indicates withdrawal of signaling factors. A: A83-01; B: bFGF; C: CHIR; I: IGF1; N: NRG1 agonist; P: Pioglitazone; V: Vitamin C; P1: passage 1; P2: passage 2. (e) The doubling time of CMCs in culture media that contained selected combinations of factors. The 3 and 4 combinations of signaling chemicals had the least doubling time of the CMCs. (f) The total cell count of CMCs after three passages in media that contained the selected factors. As presented, CMCs had the highest cell count in media that contained the 3 and 4 combinations of chemicals. All data: mean ± SD and statistically analyzed by one-way ANOVA followed by Tukey’s post-hoc test. \*P ≤ 0.05; \*\*P ≤ 0.01; #Number.

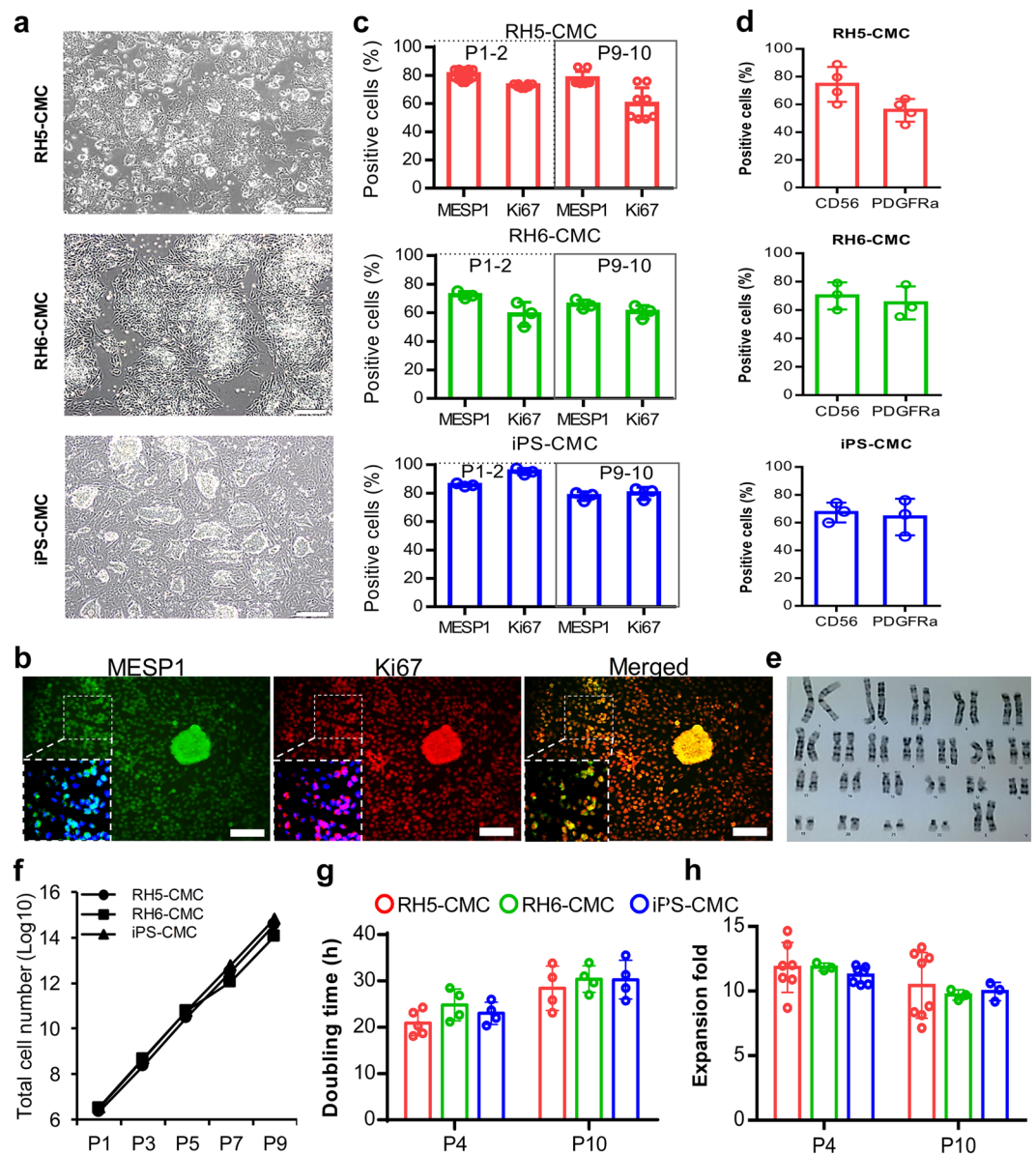


**Figure 3.** Characterization of CMCs after passages under adherent culture conditions in ABC medium. **(a)** Morphology of cultured CMCs derived from RH5, RH6, and iPS lines in ABC medium. **(b)** Immunofluorescence analysis of MESP1 and Ki67 expressions in CMCs cultured in ABC medium. Cells were counter-stained with DAPI. **(c)** Representative graphs show the percentages of MESP1<sup>+</sup> and Ki67<sup>+</sup> cells in cultured CMCs derived from RH5, RH6, and iPS lines at early (1–2) and late (9–10) passages as analyzed by flow cytometry. **(d)** PDGFRα and CD56 surface marker analysis of CMCs at the late passages. **(e)** Karyotype image of cultured RH5-derived CMCs in ABC medium at passage 10 (P10) that shows the normal cell karyotype. **(f)** Representative graph of total cell counts generated after nine passages of RH5-, RH6- and iPS-derived CMCs in ABC medium. **(g,h)** Doubling time and expansion fold of CMCs at early and late passages. Scale bars: 200 μm. All data: mean ± SD. The statistical differences between P4 and P10 in all experimental groups were analyzed by unpaired t-test.

RH6-CMC and iPS-CMC in ABC medium expressed cardiac mesoderm markers and downregulated the definitive endoderm and neural ectoderm genes (Fig. 4b,c).

In order to examine the tumorigenicity of the expanded cells in ABC medium, the early (P4), late (P10), and P0 CMCs were injected into nude mice. No sign of tumor formation was detected 90 days after the injections; however, transplantation of hPSCs led to the development of a recognizable tumor mass 20 days after the injections (Supplementary Table S2 and Supplementary Fig. S5). Taken together, these results indicated that the cells retained their original characteristics throughout passaging while the lack of tumorigenicity resolved their safety concerns.

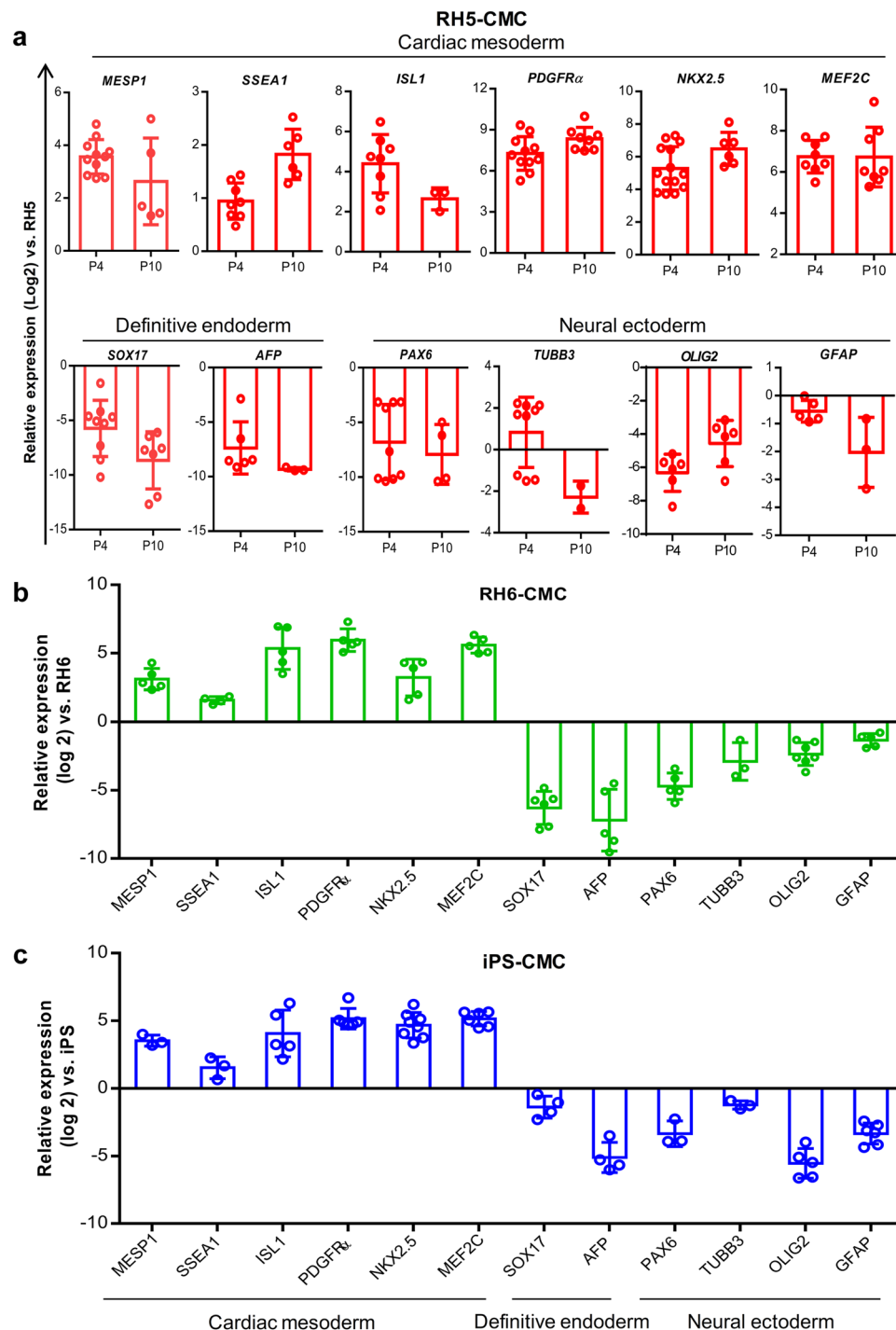


**Figure 4.** Expression pattern of cardiac mesoderm, definitive endoderm, and neural ectoderm genes in adherently expanded CMCs. Quantitative RT-PCR analysis showed upregulation of cardiac mesoderm and downregulation of definitive endoderm and neural ectoderm genes in CMCs derived from RH5 (a), RH6 (b), and iPS (c) cell lines. Analysis was performed at passage 4 (P4) for (b) and (c). All data: mean  $\pm$  SD. The statistical differences between P4 and P10 in (a) were analyzed by the unpaired t-test.

**Cryopreservation and recovery of CMCs.** A simple and efficient freeze-thaw procedure was developed to store CMCs for extended periods of time and facilitate their transportation. Cryopreserved CMCs were grown in ABC medium (Fig. 5a). More than 90% of the cells were viable immediately after thawing (Fig. 5b). Furthermore, the percentages of *MESP1*<sup>+</sup> and *Ki67*<sup>+</sup> cells were retained, even after three passages post-recovery (Fig. 5c).

**Scalable suspension culture system of CMCs.** In order to develop a scalable culture of CMCs, the adherent culture was transformed into a suspension system. Cells cultured in ABC medium in non-adhesive

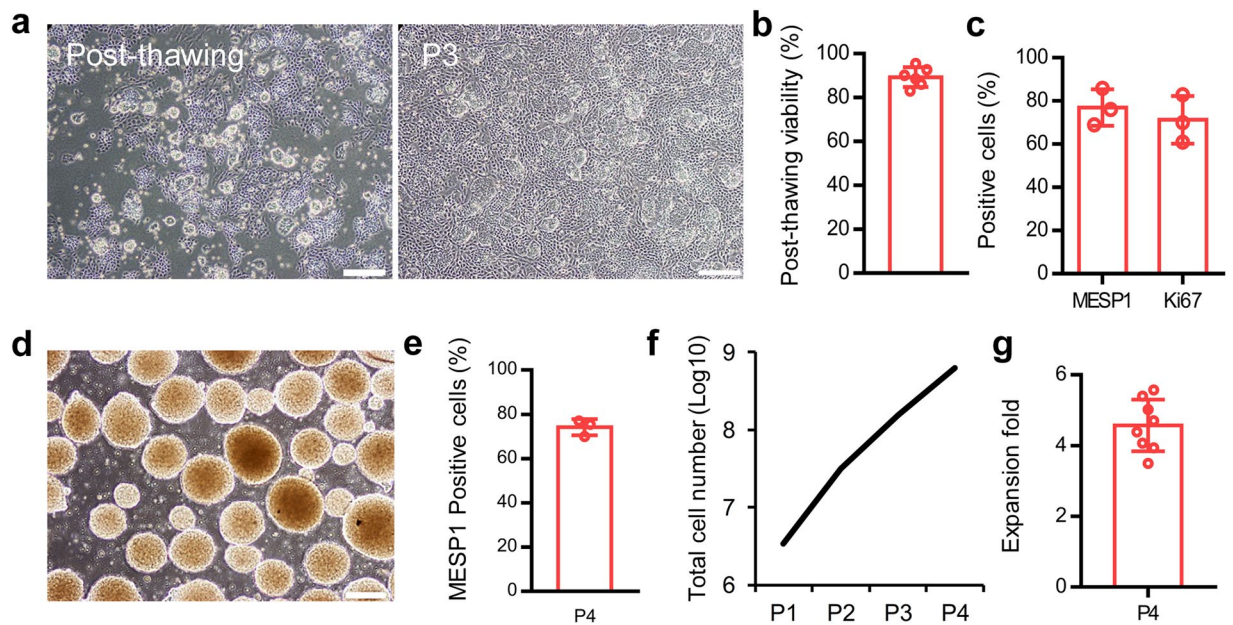


**Figure 5.** Long-term storage and suspension culture of CMCs. (a) The morphology of cryopreserved CMCs post-thaw and after three passages in ABC medium. (b) The survival rate of cryopreserved CMCs post-thaw. (c) The percentages of MESP1<sup>+</sup> and Ki67<sup>+</sup> cells in cryopreserved CMCs after three passages in ABC medium as assessed by flow cytometry. (d) The morphology of generated CMC-spheroids in ABC medium at day 4 of suspension culture. (e) The percentage of MESP1<sup>+</sup> cells after four passages of CMCs in suspension culture as evaluated by flow cytometry. (f,g) The calculated total cell count and expansion fold after four passages of CMCs in suspension culture condition. Scale bars: 200  $\mu$ m. All data: mean  $\pm$  SD.

bacterial plates acquired a spheroid shape ( $200 \pm 25 \mu\text{m}$  in diameter) four days after culture (Fig. 5d). The percentage of MESP1<sup>+</sup> cells was retained in the suspension culture condition and  $>10^8$  cells were generated after 4 passages (Fig. 5e,f). Expansion of cells at passage 4 showed greater than 4-fold cell expansion (Fig. 5g).

**Assessment of differentiation potential into main cardiac lineages.** The differentiation potential of P10 CMCs into cardiomyocytes was examined (Fig. 6a)<sup>18</sup>. The morphology of CMCs changed into elongated cells along with substantial upregulation of the cardiomyocytes' structural genes (*cTNT*, *MLC2v*, and *GJA1*) 15 days post-induction (Fig. 6b,c). Moreover, differentiated cells were positive for cTNT according to the results of immunofluorescence staining (Fig. 6d).

P10 CMCs were also induced into endothelial and smooth muscle cells (Fig. 6a)<sup>19</sup>. The cells acquired cobblestone-like morphology of endothelial and spindle shape of smooth muscle cells after induction (Fig. 6b). These differentiated cells substantially upregulated endothelial (*KDR* and *vWF*) and smooth muscle (*PDGFRa* and *MYH11*) markers 12 days post-differentiation (Fig. 6c). Immunofluorescence staining showed the presence of vWF and  $\alpha$ -SMA positive cells (Fig. 6d).

**In vivo evaluation of CMCs.** The safety and cardiac repair potential of cultured CMCs was examined *in vivo*. The adult rats received intramyocardial (IM) injections of  $4 \times 10^6$  P4 or P10 CMCs (CMC-P4 or CMC-P10) 20 min after MI induction (Fig. 7a). The animals were immunosuppressed with cyclosporine A. Their cardiac function was assessed by echocardiography. Heart performance, as assessed by ejection fraction (EF) and  $\Delta$ EF, was substantially improved two months after cell transplantation compared to the vehicle group (Fig. 7b,c). At day 60 of the follow up period, the transplanted groups had a better survival rate in comparison to the vehicle group (Fig. 7d). Masson's trichrome (MT) staining of the cardiac tissues harvested from the transplanted animals showed significantly reduced scar areas compared to the vehicle receiving group (Fig. 7e,f). The scar size of the left ventricle was significantly reduced in the CMC-P4 ( $18.0 \pm 1.9\%$ ) and CMC-P10 ( $22.2 \pm 1.5\%$ ) transplanted groups compared to the vehicle group ( $35.9 \pm 7.0\%$ ; Fig. 7g).

Moreover, there were significantly more  $\alpha$ SMA<sup>+</sup> vascular structures in the transplanted groups compared with the vehicle group (Fig. 7h,i). No sign of teratoma formation was observed in transplanted hearts 60 days after injection.

## Discussion

In this study, initially, CMCs were generated by induction of three hPSC lines using a two-day differentiation protocol based on a small molecule working as a GSK3 inhibitor (CHIR)<sup>12</sup>. CMCs exhibited the molecular signature of early CPCs (co-expression of early and late cardiac transcription factors)<sup>5,9,19,20</sup>. This co-expressed panel of genes might reflect the transition and commitment of cells from mesoderm into an early cardiovascular fate. Although it has been reported that MESP1<sup>+</sup> progenitor cells have the ability to differentiate into both cardiac and

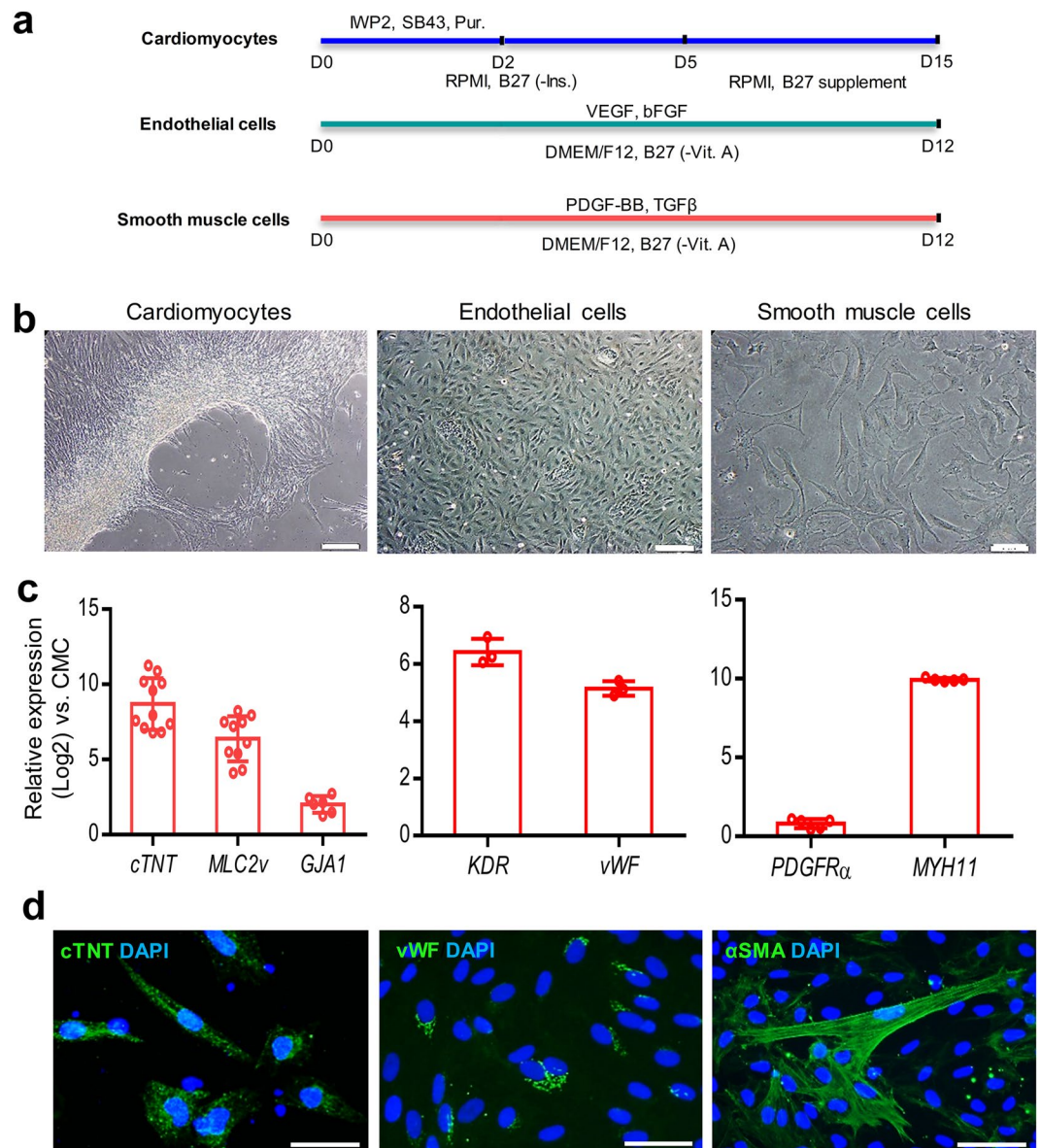


**Figure 6.** *In vitro* differentiation potential of adherently expanded CMCs in ABC medium. **(a)** Schematic illustration of induction protocols for differentiation of passage 10 CMCs into cardiomyocytes, endothelial, and smooth muscle cells. D: Day; SB43: SB431542; Pur: Purmorphamine; -Ins: Minus insulin; -Vit. A: Minus vitamin A. **(b)** Morphology of induced-CMCs into cardiomyocytes, endothelial and smooth muscle cells. Scale bars: 200  $\mu$ m. **(c)** Expression analyses of cardiomyocytes (*cTNT*, *MLC2v*, and *GJA1*), endothelial (*KDR* and *vWF*), and smooth muscle (*PDGFR $\alpha$*  and *MYH11*) cell specific genes compared to undifferentiated CMCs. All data: mean  $\pm$  SD. **(d)** Immunofluorescence staining of cTNT, vWF, and  $\alpha$ -SMA. Cells were counter-stained with DAPI. Scale bars: 100  $\mu$ m.

non-cardiac (other mesodermal) lineages<sup>21</sup>, expression of cardiac-restricted transcription factors such as *NKX2.5*, *ISL1*, and *MEF2c* might preclude the possibility of differentiation into non-cardiac cells in our culture system.

Based on the performed *in vitro* and *in vivo* developmental studies, it is accepted that *MESP1* expression is transient in the early stages of heart development and downregulated through progress of cardiogenesis<sup>15,22–25</sup>, which is consistent with the results obtained from our *in vitro* studies on hPSC-derived cardiovascular derivatives<sup>12,18</sup>. In order to develop a culture condition to expand and maintain the cells in the early stage of cardiovascular progenitors, we screened a potentially efficient pool of signaling pathway factors from a list of literature-based factors introduced as putative proliferative molecules<sup>19,26–31</sup>. Our screening resulted in the selection of A83-01, bFGF, and CHIR. Other factors as single or in combination, did not lead to expansion of CMCs. A83-01 is a potent inhibitor of TGF- $\beta$  type I receptor ALK5, nodal receptor ALK7, and activin/nodal receptor ALK4<sup>32</sup>. A83-01 can potentially be used alone or in combination with other signaling molecules for expansion of CPCs<sup>19,26,33</sup>. bFGF, a member of the fibroblast growth factor (FGF) family, is a potent mitotic factor for a wide range of cell types, including CPCs<sup>27,34</sup>. Other FGF members such as FGF8 and FGF10 have been introduced as proliferation



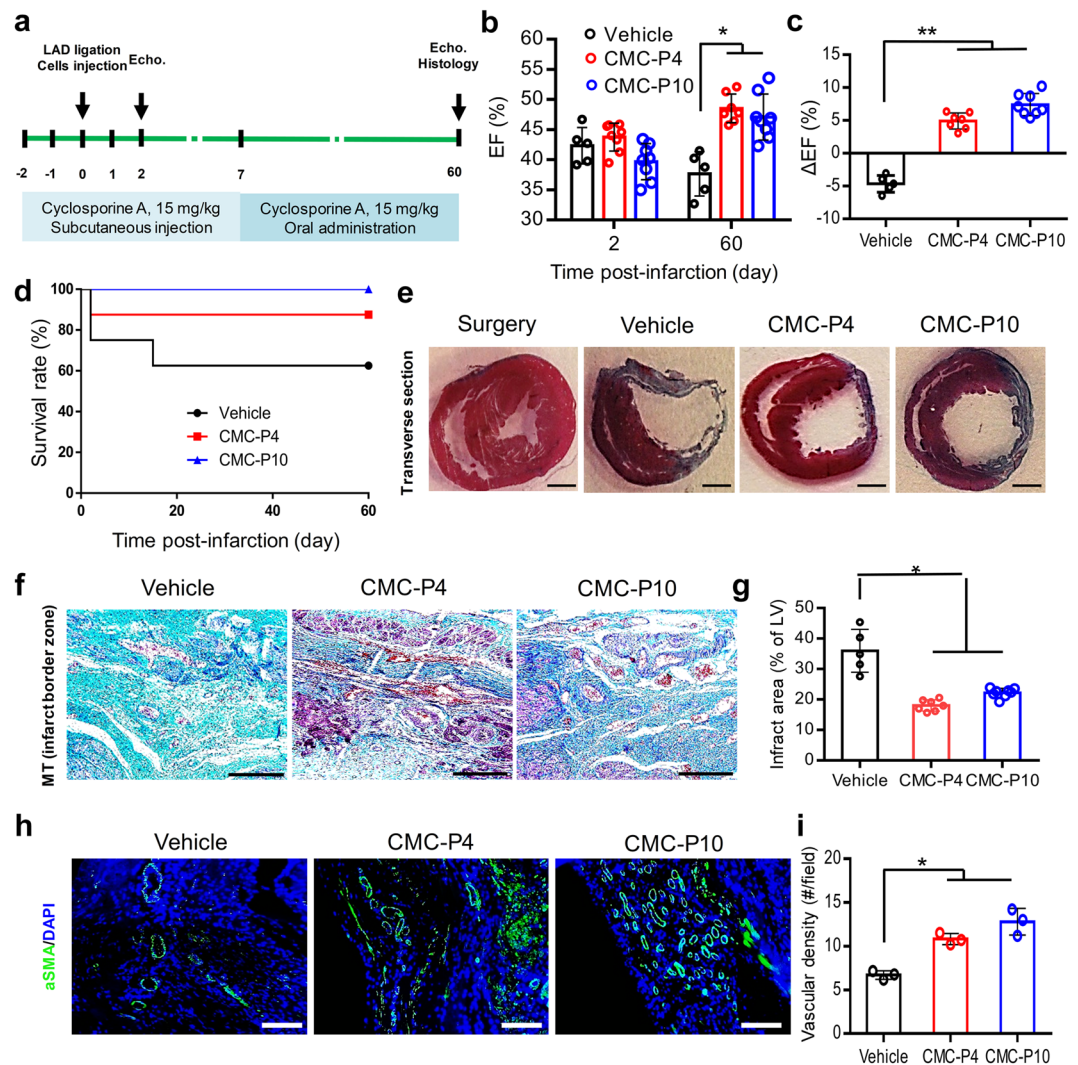


**Figure 7.** Cardio-protective effect of adherently expanded CMCs in ABC medium after transplantation into rat infarcted myocardium. **(a)** Schematic outline of the *in vivo* experiment. The animals received intramyocardial injections of the cells into the infarct border zone, 20 min after LAD artery ligation. Animals were immunosuppressed by the administration of cyclosporine A. Echo: Echocardiography. **(b)** The ejection fraction (EF) index of heart performance as evaluated by Echo at 2 and 60 days post-infarction. The data showed a significant increase of EF in the cell injected groups compared to the vehicle group. **(c)** The  $\Delta$ EF represents the difference between the EF values measured at days 2 and 60 post-infarction for the *in vivo* groups. **(d)** Kaplan-Meier survival rate analysis of different *in vivo* groups. The cell transplanted groups had a higher survival rate compared to the vehicle group. **(e)** Masson's trichrome (MT) stained transverse sections of rats' hearts 60 days after infarction. Scale bar: 2 mm. **(f)** Cardiac fibrotic tissue stained with MT at the infarct border zones. Scale bars: 200 μm. **(g)** The measured infarct fibrotic area (%) stained by MT indicated significantly decreased scar tissues in the cell transplanted groups compared to the vehicle group. **(h)** Representative immunostaining against vascular structures with anti- $\alpha$ SMA. **(i)** The quantification indicated that the significant higher vascular densities in cell transplanted groups compared to vehicle group. Scale bars: 200 μm. LV: Left ventricle. All data: mean  $\pm$  SD and statistically analyzed by one-way ANOVA followed by Tukey's post-hoc test. \* $P \leq 0.05$ ; \*\* $P \leq 0.01$ .

inducing factors in distinct CPC populations<sup>5</sup>. Of note, FGF ligands exert their roles through activation of PI3K/Akt or MAPK/ERK signaling pathways that interact downstream of other signaling pathways<sup>5,35</sup>. CHIR activates the Wnt pathway by inhibiting GSK3 signaling<sup>18</sup>. Multiple studies have shown a decisive role of the Wnt signaling pathway during embryo development, particularly cardiogenesis<sup>5,36</sup>. Therefore, a number of experiments have targeted this signaling pathway to induce expansion and improve differentiation of CPCs<sup>19,37,38</sup>. Interestingly, Wnt, TGF- $\beta$ , and PI3K/Akt signaling pathways were among the significantly enriched pathways in MESP1<sup>+</sup> cells<sup>14,39</sup>.

A proportion of cultured CMCs expressed the surface marker CD56, a proposed marker for mesodermal progenitors<sup>40,41</sup>. We have also observed expression of another surface marker in expanded CMCs, PDGFR $\alpha$ , which is a well-known CMC marker similar to MESP1<sup>42</sup>. Co-expression of PDGFR $\alpha$  and KDR has been previously used to identify the early CPCs<sup>43,44</sup>. However, the expression of KDR was downregulated in CMCs cultured in ABC

medium after passaging. Consistently, a microarray result unveiled the enrichment of *PDGFRA*, but not *KDR*, in *MESPI*<sup>+</sup> cells derived from hESCs. Flow cytometry analysis showed co-expression of *PDGFR* $\alpha$  and *MESPI* in approximately 70% of cells<sup>14</sup>. In a similar study, flow cytometry results showed rare expression of *KDR* (5–7% of the population) in *SSEA1*<sup>+</sup>*MESPI*<sup>+</sup> cells derived from differentiation of hPSCs<sup>9</sup>. Of note, there might be different subpopulations in cultured CMCs as we did not perform clonal assessments or cell sorting for cell populations resulting in high purity. Further studies are required to generate more homogeneous populations.

CMCs were expanded for approximately 11-fold at the early passages in ABC medium. This rate showed an insignificant, partial decrease in the late passages. The expansion rate, PDT, and total count of expanded cells in ABC medium were comparable with the results reported by Cao *et al.*<sup>19</sup>. Similarly, we observed a consistent cardiac gene expression profile and no detectable expression levels for the specific endoderm and ectoderm lineage markers in the CMCs during passaging<sup>19</sup>. Although this would indicate that the expanded CMCs had distinguishable gene expression signature from other cell types, a genome-wide gene expression assessment is required to provide a conclusive view in this regard.

As another characteristic of expanded CMCs in ABC medium, their *in vitro* differentiation capacity was evaluated; however, our cardiomyocyte differentiation protocol could not efficiently generate spontaneously beating cardiomyocytes; therefore, this suboptimal protocol should be further optimized. Possibly, more specific and directed differentiation protocols are required to mimic the signals generated from the cardiac niche that result in beating cardiomyocytes in order to provide the specific proofs and evidences for cardiomyogenic differentiation potential of expanded CMCs. Consistently, the expandable CPCs generated from transdifferentiation of mouse fibroblasts (named as induced CPCs; iCPCs) had differentiation potential into cardiovascular lineages as evidenced by fluorescent staining of specific markers; however, despite the existence of highly organized sarcomeres, the differentiated iCPCs into cardiomyocytes failed to spontaneously contract<sup>20</sup>.

Our *in vivo* results exhibited the safety and cardio-protection of injected CMCs in the heart with no signs of teratoma formation 60 days after injection. We showed that an IM injection of CMCs, regardless of passage number, may ameliorate heart performance 60 days post-infarction compared to the vehicle group. The improvement might be attributed to cardiac differentiation, paracrine effects, and increase in angiogenesis or cardio-protection in the acute infarct setting. The secretion of paracrine factors from CPCs has been shown<sup>33,45</sup>. In addition, alternative mechanisms could be post-MI inflammation regulation and indirect modulation of the natural immune responses to dying cells<sup>46</sup>. However, further experiments must be performed to determine the therapeutic mechanism and efficiency of CMC transplantation and CMC specific effects. Moreover, whether these mechanisms can mediate long-term repair or protection remains an open issue.

Furthermore, we established a simple, efficient protocol for long-term storage and suspension culture of CMCs to facilitate translation of our culture strategy into large-scale industrial applications. In order to increase the survival rate of CMCs after cryopreservation, we have used a potent anti-apoptotic small molecule (Rho kinase inhibitor; ROCKi, Y-27632). This is widely used, not only to circumvent the apoptosis process, but also to enhance the attachment of cells to their culture substrates<sup>34,47</sup>. We also benefited from ROCKi to improve the survival of CMCs after singularization for culture, cryopreservation, and transplantation. Another important finding of this study was the carrier-free static suspension culture and expansion of CMCs. To the best of our knowledge, this is the first report which explains the suspension culture system for expansion of hPSC-derived cardiovascular progenitors. This system facilitates the expansion of hPSC-CMC in fully controlled bioreactor systems for regenerative cell manufacturing. A study by Jha *et al.* showed higher proliferative characteristics of hPSC-derived CPCs under three-dimensional conditions stimulated by microgravity<sup>48</sup>.

In conclusion, we have introduced a culture medium that contains a combination of three signaling factors with the capability to maintain hPSC-CMCs in their proliferative progenitor state. The expanded CMCs retained the typical features of early cardiovascular progenitors with no safety concerns for tumorigenicity and might improve cardiac performance after transplantation into the infarct border zone. Moreover, they possessed the capacity for suspension culture and could be easily cryopreserved. These properties would make them suitable for use as raw materials in various applications such as cardiac cell therapy and tissue engineering. Two limitations of this study are: (1) the establishment of optimal induction protocols to efficiently differentiate expanded CMCs, *in vitro* and *in vivo* and (2) whether the regenerative capacity of CMCs is mediated through specific mechanisms for long-term repair or protection, which remains to be explored.

## Methods

**hPSC culture and CMC generation.** Two hESC lines, RH5 and RH6, and an iPSC line<sup>49</sup> were cultured and expanded in suspension culture according to a previously described protocol<sup>34</sup>. Briefly,  $2 \times 10^5$  viable single cells/ml in hPSC medium were transferred to non-adhesive bacterial plates. The medium was conditioned an overnight on human foreskin fibroblasts which were inactivated by mitomycin C (Sigma-Aldrich, M0503). The hPSC medium contained DMEM/F12 (Gibco, 31331028) supplemented with 20% knockout serum replacement (KO-SR; Gibco, 10828-028), 1% nonessential amino-acids (NEAA; Gibco, 11140-035), 1% penicillin/streptomycin (Gibco, 15070-063), 1% insulin-transferrin-selenite (ITS; Gibco, 51500-056), 0.1 mM  $\beta$ -mercaptoethanol (Sigma-Aldrich, M7522), and freshly added 100 ng/ml bFGF (Royan Biotech). Cells were treated with 10  $\mu$ M of ROCKi (Sigma-Aldrich, Y0503) for the first two days and the medium was refreshed every two days. In order to induce hPSCs into CMCs, 5-day old spheroids (175–200  $\mu$ m in diameter) were treated with 12  $\mu$ M of the small molecule, CHIR (Stemgent, 04-0004-10), in basal differentiation medium that consisted of RPMI 1640 (Gibco, 52400-041) supplemented with 2% B-27 without insulin (Gibco, A18956-01), 2 mM L-glutamine (Gibco, 25030-024), 1% NEAA, 1% penicillin/streptomycin, and 0.1 mM  $\beta$ -mercaptoethanol for one day followed by one-day culture in basal differentiation medium without small molecule<sup>12</sup>.

**Culture and maintenance of CMC.** CMC spheroids were dissociated into single cells by treatment with Accutase solution (Sigma-Aldrich, A6964) for 3 min at 37 °C and subsequently cultured at a cell density of  $5 \times 10^4$  cells/cm<sup>2</sup> on Matrigel-coated plates in basal maintenance medium that consisted of DMEM/F12 supplemented with 2% B-27 without vitamin A (Gibco, 12587-010), 2 mM L-glutamine, 1% NEAA, 0.1 mM  $\beta$ -mercaptoethanol, and freshly added chosen factors, 0.5  $\mu$ M A83-01 (Stemgent, 04-0014), 100 ng/ml bFGF, and 3  $\mu$ M CHIR, which we named ABC medium. Cells were treated overnight with 10  $\mu$ M ROCKi and the medium was refreshed daily. CMCs were routinely passaged every 4 days by using Accutase and cultured on Matrigel-coated plates at a cell density of  $5 \times 10^4$  cells/cm<sup>2</sup> in ABC medium.

**CMC characterization.** For detailed methods on CMC characterization, see supplemental information.

**In vivo assessment of CMC.** *Acute Myocardial infarction (AMI) model.* AMI was induced in adult male Wistar rats (weight: 250–300 g) according to a previously published protocol with some modifications<sup>6</sup>. Animals were housed and cared according to protocols approved by the Royan Institutional Animal Care and Use Ethical Committee in conformity with the NIH Guide for the Care and Use of Laboratory Animals. Immunosuppression was performed by subcutaneous (SC) administration of 15 mg/kg/day cyclosporine A (Novartis Pharma AG) two days before surgery to seven days post-MI. During the remainder of the experiment, the animals received 15 mg/kg/day cyclosporine A added to their drinking water. Prior to surgery, the animals were anesthetized with intraperitoneal (IP) injections of 0.1 mg/kg Medetomidine (Syva, Spain) and 75 mg/kg Ketamine (Alfasan, The Netherlands). Once anesthetized, the animals were intubated and mechanically ventilated (Harvard, USA) with a mixture of room air, oxygen, and 1% Isoflurane to maintain a deep level of anesthesia. The chest area was shaved and the surgical site was prepared via aseptic techniques. A left thoracotomy was performed to expose the left ventricle and infarction was achieved by permanent ligation of the left anterior descending artery (LAD) with 6-0 monofilament polypropylene suture material (Keyhan Teb, Iran). The AMI was established by regional color change of the myocardial surface. In this study, 30 rats were divided into four experimental groups: sham-operated (surgery; n = 6), control AMI-induced (vehicle; n = 8), and treatment (CMC-P4; n = 8 and CMC-P10; n = 8). With the exception of the sham group animals, the other rats received either 500  $\mu$ l PBS/10%BSA in the vehicle group or  $4 \times 10^6$  ROCKi treated-cells in 500  $\mu$ l PBS/10%BSA in the treatment groups. IM injections (100  $\mu$ l per injection) were administered at five sites of the infarct border zone 20 min after the LAD ligation. After the injection, the ribs, muscle layers, SC layer, and skin were closed and the animals received an IP injection of 1 mg/kg Atipamezole (Syva, Spain). The animals were placed on a heating stage until recovery. They received a prophylactic antibiotic (Enrofloxacin, 15 mg/kg, SC, Rooyan Darou, Iran) and analgesic (Tramadol, 20 mg/kg, SC, Darou Pakhsh, Iran) for three days to prevent infection and to perform pain management, respectively. At the end of the study, rats were euthanized using CO<sub>2</sub> inhalation.

**Echocardiographic assessment.** Cardiac function was evaluated in rats by echocardiographic assessment using an ultrasound system (Mindray, USA) on days 2 (baseline) and 60 after the AMI. The animals were anesthetized by IP injections of Medetomidine and Ketamine, and their chests were shaved. An experienced cardiologist blinded to the treatment groups performed the ultrasound. The data was acquired as two-dimensional images. End-diastolic and systolic volumes were obtained to assess the left ventricular EF.  $\Delta$ EF for each animal was calculated by subtracting the EF value of baseline from EF value on day 60.

**Histological studies.** Two months after surgery, the animals were sacrificed and their hearts were removed and fixed with 10% formalin at room temperature (RT) for 72 h. The processed hearts were embedded in paraffin and cut into 5  $\mu$ m thick sections. After deparaffinization and hydration, the heart sections were stained by MT to visualize the infarct area. The percentage of the infarct area was calculated with ImageJ software. We chose six slides for each animal and calculated the mean percentage of the infarct area.

For immunofluorescence staining, deparaffinized and rehydrated sections underwent antigen retrieval using Target Retrieval Solution, pH 9, (Dako, S2368) for 20 min. Thereafter, sections were permeabilized with 0.5% triton X100 at RT for 30 min, blocked for 1 h at 37 °C and then incubated overnight with primary antibodies at 4 °C. The next day, sections were washed and treated with secondary antibodies at 37 °C for 1 h, counterstained with DAPI and observed under fluorescence microscope (Olympus; IX71). To measure vascular density in infarcted regions, the number of a-SMA<sup>+</sup> vascular structures was counted in five fields per section and three sections were utilized for each animal<sup>6</sup>.

**Freeze-thaw procedure.** For long-term storage of CMCs, we used Accutase to dissociate the spheroids into single cells. After centrifugation at 1500 rpm for 5 min,  $2 \times 10^6$  cells were dissolved in 500  $\mu$ l cold freezing medium that contained 90% FBS, 10% DMSO, and 10  $\mu$ M ROCKi. Cells were kept overnight in a –80 °C freezer and transferred to a liquid nitrogen tank the next day. In order to recover the cryopreserved cells, the frozen vials were held in a 37 °C water bath until most of the ice thawed. Fresh medium that contained 10  $\mu$ M ROCKi was added to cells and, after centrifugation, the cells were resuspended in ABC medium that contained 10  $\mu$ M ROCKi and cultured on Matrigel-coated plates. Trypan blue exclusion method was used to calculate cell viability as previously described<sup>12</sup>.

**Suspension culture.** In this experiment, single CMCs were cultured at a density of  $2 \times 10^5$  cells/ml in ABC medium that contained 10  $\mu$ M ROCKi in non-adhesive bacterial plates. The medium was refreshed 2 days later with fresh ABC medium without ROCKi and renewed every two days. Spheroids generated from the expanded CMCs, with 200–250  $\mu$ m diameter, were passaged.

**Statistical analysis.** All data are presented as median or mean  $\pm$  standard deviation (SD) (obtained from at least three independent replicates). After testing the normal distribution of data, the significance of differences were statistically analyzed by SPSS 16.0 (SPSS, Inc.) using the unpaired t-test or one-way ANOVA followed by Tukey's post-hoc test. A P-value of  $\leq 0.05$  was considered to be statistically significant.

### Data availability

The datasets generated during and/or analysed during the current study are available from the corresponding author on reasonable request.

Received: 9 May 2019; Accepted: 16 October 2019;

Published online: 05 November 2019

### References

- Perricone, A. J. & Vander Heide, R. S. Novel therapeutic strategies for ischemic heart disease. *Pharmacological research* **89**, 36–45, <https://doi.org/10.1016/j.phrs.2014.08.004> (2014).
- Balistreri, C. R. *et al.* Are Endothelial Progenitor Cells the Real Solution for Cardiovascular Diseases? Focus on Controversies and Perspectives. *BioMed research international* **2015**, 835934, <https://doi.org/10.1155/2015/835934> (2015).
- Nigro, P. *et al.* Cell therapy for heart disease after 15 years: Unmet expectations. *Pharmacological research* **127**, 77–91, <https://doi.org/10.1016/j.phrs.2017.02.015> (2018).
- Chen, C., Termglinchan, V. & Karakikes, I. Concise Review: Mending a Broken Heart: The Evolution of Biological Therapeutics. *Stem cells* **35**, 1131–1140, <https://doi.org/10.1002/stem.2602> (2017).
- Birket, M. J. & Mummery, C. L. Pluripotent stem cell derived cardiovascular progenitors—a developmental perspective. *Developmental biology* **400**, 169–179, <https://doi.org/10.1016/j.ydbio.2015.01.012> (2015).
- Vahdat, S. *et al.* Cellular and molecular characterization of human cardiac stem cells reveals key features essential for their function and safety. *Stem cells and development* **24**, 1390–1404, <https://doi.org/10.1089/scd.2014.0222> (2015).
- Wu, S. M., Chien, K. R. & Mummery, C. Origins and fates of cardiovascular progenitor cells. *Cell* **132**, 537–543, <https://doi.org/10.1016/j.cell.2008.02.002> (2008).
- Bellamy, V. *et al.* Long-term functional benefits of human embryonic stem cell-derived cardiac progenitors embedded into a fibrin scaffold. *The Journal of heart and lung transplantation: the official publication of the International Society for Heart Transplantation* **34**, 1198–1207, <https://doi.org/10.1016/j.healun.2014.10.008> (2015).
- Blin, G. *et al.* A purified population of multipotent cardiovascular progenitors derived from primate pluripotent stem cells engrafts in postmyocardial infarcted nonhuman primates. *The Journal of clinical investigation* **120**, 1125–1139, <https://doi.org/10.1172/JCI40120> (2010).
- Zhu, K. *et al.* Lack of Remuscularization Following Transplantation of Human Embryonic Stem Cell-Derived Cardiovascular Progenitor Cells in Infarcted Nonhuman Primates. *Circulation research* **122**, 958–969, <https://doi.org/10.1161/CIRCRESAHA.117.311578> (2018).
- Menasche, P. *et al.* Transplantation of Human Embryonic Stem Cell-Derived Cardiovascular Progenitors for Severe Ischemic Left Ventricular Dysfunction. *J Am Coll Cardiol* **71**, 429–438, <https://doi.org/10.1016/j.jacc.2017.11.047> (2018).
- Vahdat, S., Pahlavan, S., Aghdami, N., Bakhshandeh, B. & Baharvand, H. Establishment of A Protocol for *In Vitro* Culture of Cardiogenic Mesodermal Cells Derived from Human Embryonic Stem Cells. *Cell journal* **20**, 496–504, <https://doi.org/10.22074/cellj.2019.5661> (2019).
- Brade, T., Pane, L. S., Moretti, A., Chien, K. R. & Laugwitz, K. L. Embryonic heart progenitors and cardiogenesis. *Cold Spring Harb Perspect Med* **3**, a013847, <https://doi.org/10.1101/cshperspect.a013847> (2013).
- Den Hartogh, S. C. *et al.* Dual reporter MESP1 mCherry/w-NKX2-5 eGFP/w hESCs enable studying early human cardiac differentiation. *Stem cells* **33**, 56–67, <https://doi.org/10.1002/stem.1842> (2015).
- Bondue, A. *et al.* Mesp1 acts as a master regulator of multipotent cardiovascular progenitor specification. *Cell stem cell* **3**, 69–84, <https://doi.org/10.1016/j.stem.2008.06.009> (2008).
- Lescroart, F. *et al.* Defining the earliest step of cardiovascular lineage segregation by single-cell RNA-seq. *Science* **359**, 1177–1181, <https://doi.org/10.1126/science.aao4174> (2018).
- Liu, Y. Earlier and broader roles of Mesp1 in cardiovascular development. *Cell Mol Life Sci* **74**, 1969–1983, <https://doi.org/10.1007/s00018-016-2448-y> (2017).
- Fonoudi, H. *et al.* A Universal and Robust Integrated Platform for the Scalable Production of Human Cardiomyocytes From Pluripotent Stem Cells. *Stem cells translational medicine* **4**, 1482–1494, <https://doi.org/10.5966/sctm.2014-0275> (2015).
- Cao, N. *et al.* Highly efficient induction and long-term maintenance of multipotent cardiovascular progenitors from human pluripotent stem cells under defined conditions. *Cell research* **23**, 1119–1132, <https://doi.org/10.1038/cr.2013.102> (2013).
- Lalit, P. A. *et al.* Lineage Reprogramming of Fibroblasts into Proliferative Induced Cardiac Progenitor Cells by Defined Factors. *Cell stem cell* **18**, 354–367, <https://doi.org/10.1016/j.stem.2015.12.001> (2016).
- Chan, S. S. *et al.* Mesp1 patterns mesoderm into cardiac, hematopoietic, or skeletal myogenic progenitors in a context-dependent manner. *Cell stem cell* **12**, 587–601, <https://doi.org/10.1016/j.stem.2013.03.004> (2013).
- Paige, S. L., Plonowska, K., Xu, A. & Wu, S. M. Molecular regulation of cardiomyocyte differentiation. *Circulation research* **116**, 341–353, <https://doi.org/10.1161/CIRCRESAHA.116.302752> (2015).
- Saga, Y. *et al.* MesP1: a novel basic helix-loop-helix protein expressed in the nascent mesodermal cells during mouse gastrulation. *Development* **122**, 2769–2778 (1996).
- Saga, Y. *et al.* MesP1 is expressed in the heart precursor cells and required for the formation of a single heart tube. *Development* **126**, 3437–3447 (1999).
- Saga, Y., Kitajima, S. & Miyagawa-Tomita, S. Mesp1 expression is the earliest sign of cardiovascular development. *Trends in cardiovascular medicine* **10**, 345–352 (2000).
- Chen, W. P. & Wu, S. M. Small molecule regulators of postnatal Nkx2.5 cardiomyoblast proliferation and differentiation. *Journal of cellular and molecular medicine* **16**, 961–965, <https://doi.org/10.1111/j.1582-4934.2011.01513.x> (2012).
- Drowley, L. *et al.* Human Induced Pluripotent Stem Cell-Derived Cardiac Progenitor Cells in Phenotypic Screening: A Transforming Growth Factor-beta Type 1 Receptor Kinase Inhibitor Induces Efficient Cardiac Differentiation. *Stem cells translational medicine* **5**, 164–174, <https://doi.org/10.5966/sctm.2015-0114> (2016).
- Engels, M. C. *et al.* Insulin-like growth factor promotes cardiac lineage induction *in vitro* by selective expansion of early mesoderm. *Stem cells* **32**, 1493–1502, <https://doi.org/10.1002/stem.1660> (2014).
- Formiga, F. R. *et al.* Controlled delivery of fibroblast growth factor-1 and neuregulin-1 from biodegradable microparticles promotes cardiac repair in a rat myocardial infarction model through activation of endogenous regeneration. *Journal of controlled release: official journal of the Controlled Release Society* **173**, 132–139, <https://doi.org/10.1016/j.jconrel.2013.10.034> (2014).

30. Zadegan, F. G. *et al.* Cardiac differentiation of mouse embryonic stem cells is influenced by a PPAR gamma/PGC-1alpha-FNDC5 pathway during the stage of cardiac precursor cell formation. *European journal of cell biology* **94**, 257–266, <https://doi.org/10.1016/j.ejcb.2015.04.002> (2015).
31. Cao, N. *et al.* Ascorbic acid enhances the cardiac differentiation of induced pluripotent stem cells through promoting the proliferation of cardiac progenitor cells. *Cell research* **22**, 219–236, <https://doi.org/10.1038/cr.2011.195> (2012).
32. Tojo, M. *et al.* The ALK-5 inhibitor A-83-01 inhibits Smad signaling and epithelial-to-mesenchymal transition by transforming growth factor-beta. *Cancer science* **96**, 791–800, <https://doi.org/10.1111/j.1349-7006.2005.00103.x> (2005).
33. Ho, Y. S. *et al.* Cardioprotective Actions of TGFbetaRI Inhibition Through Stimulating Autocrine/Paracrine of Survivin and Inhibiting Wnt in Cardiac Progenitors. *Stem cells* **34**, 445–455, <https://doi.org/10.1002/stem.2216> (2016).
34. Larijani, M. R. *et al.* Long-term maintenance of undifferentiated human embryonic and induced pluripotent stem cells in suspension. *Stem cells and development* **20**, 1911–1923, <https://doi.org/10.1089/scd.2010.0517> (2011).
35. Luo, W. *et al.* Akt1 signaling coordinates BMP signaling and beta-catenin activity to regulate second heart field progenitor development. *Development* **142**, 732–742, <https://doi.org/10.1242/dev.119016> (2015).
36. Klaus, A., Saga, Y., Taketo, M. M., Tzahor, E. & Birchmeier, W. Distinct roles of Wnt/beta-catenin and Bmp signaling during early cardiogenesis. *Proceedings of the National Academy of Sciences of the United States of America* **104**, 18531–18536, <https://doi.org/10.1073/pnas.0703113104> (2007).
37. Kwon, C. *et al.* A regulatory pathway involving Notch1/beta-catenin/Is1 determines cardiac progenitor cell fate. *Nature cell biology* **11**, 951–957, <https://doi.org/10.1038/ncb1906> (2009).
38. Qyang, Y. *et al.* The renewal and differentiation of Isl1+ cardiovascular progenitors are controlled by a Wnt/beta-catenin pathway. *Cell stem cell* **1**, 165–179, <https://doi.org/10.1016/j.stem.2007.05.018> (2007).
39. Vahdat, S. & Bakhshandeh, B. Prediction of putative small molecules for manipulation of enriched signalling pathways in hESC-derived early cardiovascular progenitors by bioinformatics analysis. *IET Systems Biology* **13**, 77–83 (2018).
40. den Hartogh, S. C., Wolstencroft, K., Mummery, C. L. & Passier, R. A comprehensive gene expression analysis at sequential stages of *in vitro* cardiac differentiation from isolated MESP1-expressing-mesoderm progenitors. *Scientific reports* **6**, 19386, <https://doi.org/10.1038/srep19386> (2016).
41. Evseenko, D. *et al.* Mapping the first stages of mesoderm commitment during differentiation of human embryonic stem cells. *Proceedings of the National Academy of Sciences of the United States of America* **107**, 13742–13747, <https://doi.org/10.1073/pnas.1002077107> (2010).
42. Chen, V. C. *et al.* Development of a scalable suspension culture for cardiac differentiation from human pluripotent stem cells. *Stem cell research* **15**, 365–375, <https://doi.org/10.1016/j.scr.2015.08.002> (2015).
43. Ardehali, R. *et al.* Prospective isolation of human embryonic stem cell-derived cardiovascular progenitors that integrate into human fetal heart tissue. *Proceedings of the National Academy of Sciences of the United States of America* **110**, 3405–3410, <https://doi.org/10.1073/pnas.1220832110> (2013).
44. Kattman, S. J. *et al.* Stage-specific optimization of activin/nodal and BMP signaling promotes cardiac differentiation of mouse and human pluripotent stem cell lines. *Cell stem cell* **8**, 228–240, <https://doi.org/10.1016/j.stem.2010.12.008> (2011).
45. Kervadec, A. *et al.* Cardiovascular progenitor-derived extracellular vesicles recapitulate the beneficial effects of their parent cells in the treatment of chronic heart failure. *The Journal of heart and lung transplantation: the official publication of the International Society for Heart Transplantation* **35**, 795–807, <https://doi.org/10.1016/j.healun.2016.01.013> (2016).
46. Wang, J. *et al.* Human Embryonic Stem Cell-Derived Cardiovascular Progenitors Repair Infarcted Hearts Through Modulation of Macrophages via Activation of Signal Transducer and Activator of Transcription 6. *Antioxidants & redox signaling* **31**, 369–386, <https://doi.org/10.1089/ars.2018.7688> (2019).
47. Pakzad, M. *et al.* Presence of a ROCK inhibitor in extracellular matrix supports more undifferentiated growth of feeder-free human embryonic and induced pluripotent stem cells upon passaging. *Stem cell reviews* **6**, 96–107, <https://doi.org/10.1007/s12015-009-9103-z> (2010).
48. Jha, R. *et al.* Simulated Microgravity and 3D Culture Enhance Induction, Viability, Proliferation and Differentiation of Cardiac Progenitors from Human Pluripotent Stem Cells. *Scientific reports* **6**, 30956, <https://doi.org/10.1038/srep30956> (2016).
49. Seifinejad, A. *et al.* Generation of human induced pluripotent stem cells from a Bombay individual: moving towards “universal-donor” red blood cells. *Biochemical and biophysical research communications* **391**, 329–334, <https://doi.org/10.1016/j.brc.2009.11.058> (2010).

## Acknowledgements

The authors would like to thank Payam Taheri, Elham Kordestani, Paria Pooyan, Najmeh Sadat Masoudi, and Shaghayegh Vahdat for their time and assistance. This work was supported by a grant from Royan Institute, the Iranian Council of Stem Cell Research and Technology, the Iran National Science Foundation (INSF, grant no. 96001316), and Iran Science Elites Federation to H.B.

## Author contributions

S.V.: Contributed to all experimental work, data analysis and paper draft preparation. S.P.: Paper draft preparation and edition. E.M. (veterinary surgeon): Performed the animal-related surgeries. M.B. (cardiologist): Assayed cardiac function of the animal models. H.A.: Provided the differentiated cells. B.B.: Scientific supervisor of the project and finalized the manuscript. N.A.: Scientific adviser of the project. H.B.: Scientific supervisor of the project, provided the main idea, and finalized the manuscript. All authors approved the final version of this manuscript.

## Competing interests

The authors declare no competing interests.

## Additional information

**Supplementary information** is available this paper at <https://doi.org/10.1038/s41598-019-52516-8>.

**Correspondence** and requests for materials should be addressed to H.B.

**Reprints and permissions information** is available at [www.nature.com/reprints](http://www.nature.com/reprints).

**Publisher's note** Springer Nature remains neutral with regard to jurisdictional claims in published maps and institutional affiliations.



**Open Access** This article is licensed under a Creative Commons Attribution 4.0 International License, which permits use, sharing, adaptation, distribution and reproduction in any medium or format, as long as you give appropriate credit to the original author(s) and the source, provide a link to the Creative Commons license, and indicate if changes were made. The images or other third party material in this article are included in the article's Creative Commons license, unless indicated otherwise in a credit line to the material. If material is not included in the article's Creative Commons license and your intended use is not permitted by statutory regulation or exceeds the permitted use, you will need to obtain permission directly from the copyright holder. To view a copy of this license, visit <http://creativecommons.org/licenses/by/4.0/>.

© The Author(s) 2019